nature nanotechnology

LETTERS

PUBLISHED ONLINE: 1 APRIL 2012 | DOI: 10.1038/NNANO.2012.42

A nanomechanical mass sensor with yoctogram resolution

J. Chaste[1], A. Eichler[1], J. Moser[1], G. Ceballos[1], R. Rurali[2] and A. Bachtold[1]*

Nanomechanical resonators have been used to weigh cells, biomolecules and gas molecules[1–4], and to study basic phenomena in surface science, such as phase transitions[5] and diffusion[6,7]. These experiments all rely on the ability of nanomechanical mass sensors to resolve small masses. Here, we report mass sensing experiments with a resolution of 1.7 yg (1 yg = 10^{-24} g), which corresponds to the mass of one proton. The resonator is a carbon nanotube of length ∼150 nm that vibrates at a frequency of almost 2 GHz. This unprecedented level of sensitivity allows us to detect adsorption events of naphthalene molecules ($C_{10}H_8$), and to measure the binding energy of a xenon atom on the nanotube surface. These ultrasensitive nanotube resonators could have applications in mass spectrometry, magnetometry and surface science.

The operation of a nanomechanical mass sensor relies on monitoring how the resonance frequency of a nanomechanical resonator changes when additional mass is adsorbed onto its surface. Theoretical analysis predicts that a sensitivity comparable to the mass of one proton should be feasible[8,9], which would open up the possibility of distinguishing between different chemical elements in future inertial mass spectrometry measurements. However, so far, the best mass resolution achieved with microfabricated resonators has been 7,000 yg (ref. 10), whereas carbon nanotube resonators have achieved mass resolutions as low as ∼200 yg (refs 11–13, as estimated in ref. 2).

We combined, within a single experiment, all the ingredients known to favour the detection of small masses, such as the use of a short nanotube, low-noise motion detection and ultrahigh vacuum. The device consists of a nanotube suspended over a ∼150-nm-wide trench (Fig. 1a,b). Such a short nanotube produces a sizeable change in resonance frequency, even when a tiny number of atoms are deposited on the nanotube. The motion of the nanotube was driven and detected using the frequency modulation (FM) mixing technique at liquid-helium temperature, a method known to transduce the nanotube motion into a low-noise electrical signal[14,15]. Figure 1c,d shows that the resonance frequency is very high (nearly 2 GHz) and can be tuned with a voltage V_g applied to the gate[16–18]. We developed a computer-controlled feedback loop to monitor the resonance frequency f_0 with a feedback time as short as 15 ms; alternatively, the time trace of f_0 was obtained by continuously scanning the resonance. The measurement set-up was prepared by lowering the base pressure to $\sim 3 \times 10^{-11}$ mbar to minimize adsorption of unwanted molecules. The expected time between two impinging events is ∼3,200 s (Supplementary Section A).

Key to improving the mass sensitivity is annealing the nanotube by passing a large current through it. Before annealing, the resonance frequency fluctuates between multiple levels (Fig. 1e, bottom trace). This behaviour, observed in all our resonators, has not been reported previously, probably because these fluctuations are very small. We found that annealing the nanotube with a current of ∼8 μA for ∼300 s dramatically reduced these fluctuations (Fig. 1e, top trace). We attribute the origin of these multiple-level fluctuations to a few contaminating molecules diffusing on the nanotube surface between various trapping sites (see Supplementary Section D for details). Passing a large current removes these molecules. Another advantage of current annealing is that it brings the nanotube back to its initial state after each mass sensing experiment. We continuously tested the device in Fig. 1 over a period of nine months and observed only a minor degradation in sensitivity over time. This current-induced cleaning process is possible because nanotubes are mechanically robust and chemically inert, and therefore can sustain the large current necessary for cleaning. Resonators made from other materials are usually damaged at such large current densities.

The current annealing cleaning process allows us to achieve a mass resolution of 1.7(±0.5) yg. The inset of Fig. 2 shows that the fluctuations in f_0 are remarkably low. The standard deviation δf_0 is a function of the averaging time τ,

$$\delta f_0 = \left[\frac{1}{N-1} \cdot \sum_{i=1}^{N} (\langle f_i^\tau \rangle - \langle f_0 \rangle)^2 \right]^{1/2}$$

where $\langle f_i^\tau \rangle$ is the resonance frequency averaged over the time interval i with duration τ, $\langle f_0 \rangle$ is the resonance frequency averaged over the whole measurement and N is the number of time intervals (Fig. 2). Using $\delta m = 2m_{\mathrm{eff}}\delta f_0/f_0$ together with the effective mass $m_{\mathrm{eff}} = 3(\pm 0.8) \times 10^{-19}$ g (estimated from the length and diameter of the nanotube; Supplementary Section B), we obtain a mass resolution of 1.7(±0.5) yg after 2 s averaging time. This ultralow value corresponds to approximately the mass of one proton (1.67 yg). The error in δm reflects the uncertainty in the estimation of the length and the diameter of the nanotube, obtained by atomic force microscopy (AFM).

This ultrasensitive resonator allows us to monitor the adsorption of atoms and molecules with very high levels of accuracy. On dosing (that is, sending xenon atoms through a pinhole microdoser), the resonance frequency showed a tendency to decrease (Fig. 3a), indicating that xenon atoms were being adsorbed on the nanotube. On top of this trend, abrupt upward shifts in f_0 as high as ∼5 MHz were also detected (red arrows). When we stopped dosing, no abrupt upward shift was observed (Fig. 3a). A possible origin of these upward shifts might be related to individual (or packets of) xenon atoms that either desorb into the vacuum or diffuse along the nanotube towards the clamping regions (Fig. 1a). The desorption–diffusion process may be assisted by the impact of high-energy xenon atoms (originating from a 300 K reservoir), the energies of which follow a Boltzmann distribution (because the system is out of equilibrium in such a scenario, it is difficult to discriminate between desorption and diffusion events). We carried out 45

[1]Catalan Institute of Nanotechnology, CIN2(ICN-CSIC), Campus de la UAB, 08193 Bellaterra, Barcelona, Spain, [2]Institut de Ciència de Materials de Barcelona (ICMAB-CSIC), Campus de la UAB, 08193 Bellaterra, Barcelona, Spain. *e-mail: adrian.bachtold@cin2.es

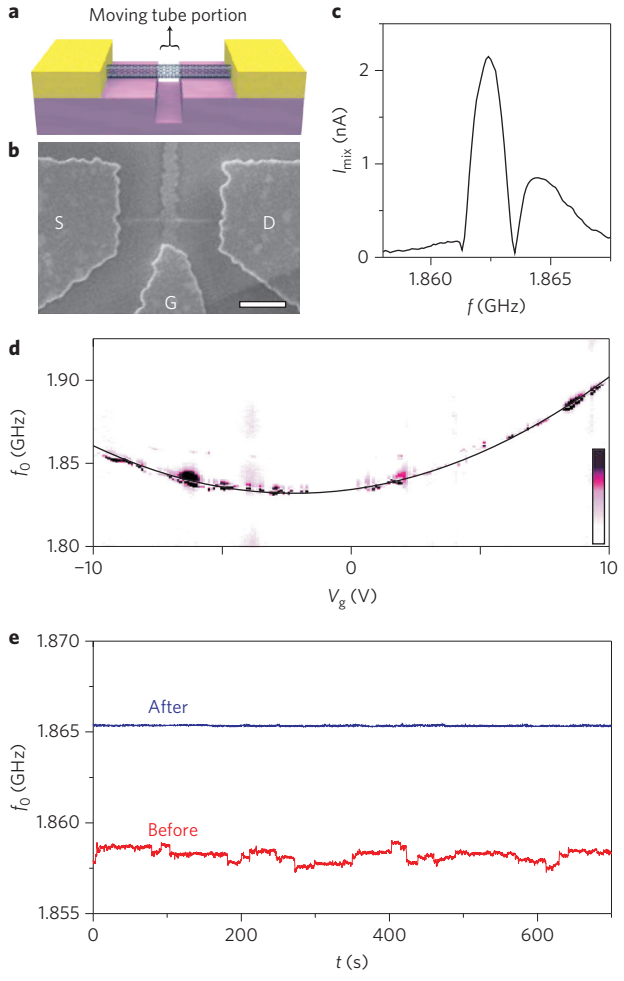

Figure 1 | Device and characterization. a,**b**, Schematic (**a**) and scanning electron microscope image (**b**) of the device (diameter of nanotube, $d = 1.7$ nm; length of suspended nanotube section, $L_{tube} \approx 150$ nm, measured with an AFM). Scale bar, 300 nm. **c**, Mechanical resonance obtained by measuring the mixing current I_{mix} as a function of driving frequency f using the FM mixing technique at 6 K (amplitude of applied FM voltage, 4 mV; integration time of the lock-in amplifier used to measure I_{mix}, 30 ms). The separation in frequency between two data points is 100 kHz. The curve has not been smoothed. The resonance is asymmetric (the lobe on the right side of the central peak is larger than the lobe on the left side); this asymmetry is attributed to the Duffing force, because it is less pronounced at lower driving forces[15]. Hysteresis jumps are not observed even at higher driving forces[15]. This resonance probably corresponds to the fundamental eigenmode, as it is the resonance with the lowest frequency and the highest I_{mix} (we detect a second resonance at 3.4 GHz). **d**, Resonance frequency f_0 as a function of the voltage applied on the side-gate electrode at 6 K; f_0 is obtained by measuring I_{mix} (which varies between 0 and 0.4 nA; see colour bar) as a function of f and V_g. I_{mix} varies with V_g because of the variation of the transconductance. **e**, Resonance frequency as a function of time at 6 K before and after current annealing. After the annealing process, we do not observe a degradation of the time trace of f_0 over at least 2,100 s (which corresponds to the longest time interval before dosing atoms).

similar measurements with xenon and naphthalene, and all showed a similar trend (Supplementary Section E).

We also observed downward shifts in f_0 that are consistent with single adsorption events. Figure 3b presents a series of such shifts obtained by dosing naphthalene ($C_{10}H_8$) molecules. The average frequency shift is -3×10^5 Hz, and a shift occurs every 1–2 s. This is in agreement with the expected average frequency shift

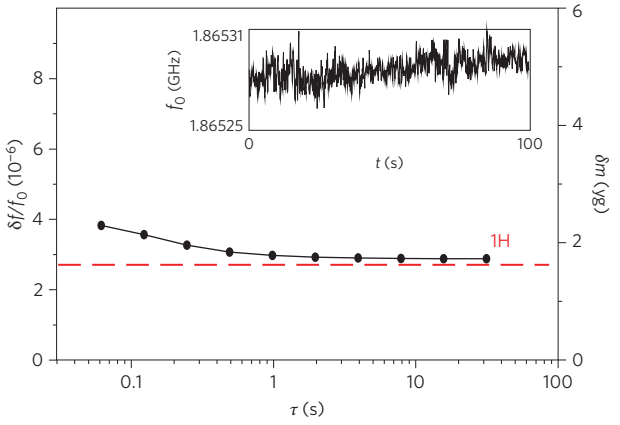

Figure 2 | Measuring mass resolution. Standard error of the resonance frequency (left axis) and corresponding mass resolution (right axis) as a function of averaging time at 5.5 K. The red dashed line corresponds to the mass of one hydrogen atom. Inset: resonance frequency as a function of time. The amplitude of the applied FM voltage is 4 mV. The current–frequency conversion used in the computer-controlled feedback loop is 0.29 kHz pA^{-1}.

$(-m_{C10H8}/2m_{NT}f_0 = -3.2 \times 10^5$ Hz) due to the adsorption of a single $C_{10}H_8$ molecule (m_{C10H8} is the mass of one $C_{10}H_8$ molecule and m_{NT} is the mass of the nanotube; Supplementary Section B). Deviations from this value are attributed to the dependence of the frequency shift on the location of the adsorption along the nanotube axis (Fig. 3b, inset). We estimate the adsorption rate from the geometry of the chamber and the measured pressure. An adsorption event is expected to occur on average approximately every 3 s, which is consistent with the measurements. Data points are missing just after large frequency shifts in Fig. 3b, because the computer-controlled feedback loop needs time to retrieve the resonance (by scanning the frequency near the previously recorded f_0; Supplementary Section A). Because of the dominant effect of desorption–diffusion, observing a series of frequency shifts as in Fig. 3b is rare. Future work will be devoted to engineering a single trapping site in the nanotube. We note that single adsorption events have previously been detected for biomolecules and nanoparticles[2] that are at least two orders of magnitude heavier than $C_{10}H_8$ molecules. Because the interaction between these large objects and the resonator is strong, their immobilization is possible without a trapping site.

We next demonstrate that the adsorption of xenon atoms onto a nanotube surface is a thermally activated process. The lower inset of Fig. 4a shows the temperature dependence of f_0 while dosing xenon atoms onto the nanotube at a rate of ~22 atoms per second. At temperatures above $T \approx 58$ K, the resonance frequency remains unchanged. On lowering the temperature, f_0 decreases. The number of xenon atoms per carbon atom is extracted using $N_{Xe}/N_C = m_C/m_{Xe} \cdot (f_{high}^2/f_0^2 - 1)$, where f_{high} is the resonance frequency at high temperature (59 K) and m_C (m_{Xe}) is the mass of a carbon (xenon) atom[5] (f_0 is essentially insensitive to the tension induced by the Xe–Xe interaction, which is two orders of magnitude weaker than the covalent C–C bonds[5]). Figure 4a shows that the temperature dependence of N_{Xe}/N_C is consistent with a thermally activated behaviour. We attribute this behaviour to the balance of xenon atoms impinging on and departing from the nanotube; on lowering T, the number of atoms on the nanotube increases as $N_{Xe} \propto \exp(E_b/k_B T)$ where E_b is the binding energy (Supplementary Section F).

We extract the xenon–nanotube binding energy ($E_b = 131$ meV) from the slope in Fig. 4a. Carrying out the measurements for a second resonator yields $E_b = 110$ meV. This energy is significantly lower than the xenon–graphite binding energy, which is 162 meV

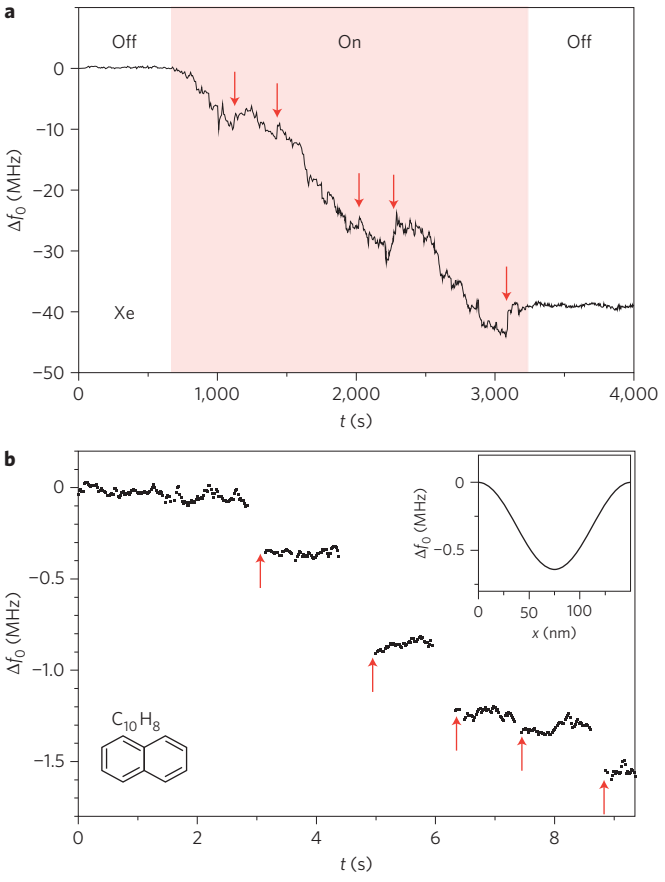

Figure 3 | Adsorption of xenon atoms and naphthalene molecules. **a,** The change in the resonance frequency Δf_0 as a function of time at 6 K as xenon atoms are being dosed onto the nanotube. Red arrows indicate some of the abrupt upward shifts discussed in the main text. The shaded area corresponds to the time when xenon atoms are dosed. Xenon atoms arrive directly from the microdoser onto the nanotube so the dosing rate cannot be estimated (Supplementary Section A). The resonance frequency is obtained by continuously measuring I_{mix} as a function of f. **b**, Δf_0 versus time at 4.3 K when naphthalene molecules are being dosed. Red arrows point to the shifts of the resonance frequency consistent with the adsorption of $C_{10}H_8$ molecules. The resonance frequency is measured using the computer-controlled feedback loop; the current–frequency conversion is 0.4 kHz pA^{-1}. Inset: expected shift in f_0 as a function of the position of the $C_{10}H_8$ adsorption along the 150-nm-long nanotube. Xenon atoms and $C_{10}H_8$ molecules are admitted from a gas reservoir at 300 K into the vacuum chamber through a pinhole microdoser. In the case of $C_{10}H_8$ dosing, unwanted contaminants are removed by freeze–pump cycles of the gas reservoir before adsorption experiments[29].

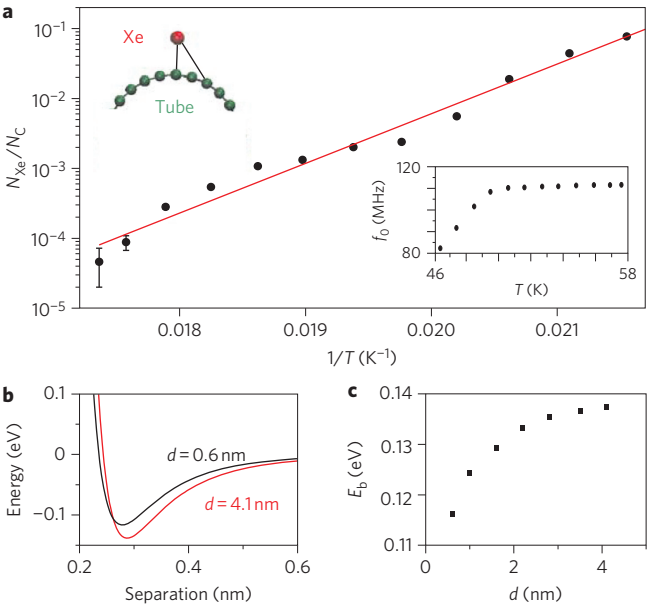

Figure 4 | Binding energy between a xenon atom and a nanotube. a, Number of xenon atoms per carbon atom as a function of $1/T$ when dosing xenon atoms onto the nanotube at a rate of ~22 atoms per second. The red line is a linear fit of the data. Lower inset: resonance frequency as a function of temperature. The device is different from the one used in Figs 1–3; the nanotube was grown in the last fabrication step over a predefined trench separating two electrodes[15,28] (diameter of nanotube, $d = 2.2$ nm; length of suspended nanotube section, $L_{tube} = 2{,}200$ nm, measured with AFM on the nanotube section lying on the electrodes). Upper inset: a xenon atom interacting with the carbon atoms of a nanotube. Note that the temperature dependence of N_{Xe}/N_C is expected to follow a thermal activation behaviour over a limited temperature range. $N_{Xe}/N_C = 1 \times 10^{-5}$ corresponds to approximately one xenon atom, and a monolayer of xenon atoms forms at $N_{Xe}/N_C = 0.1$–1. **b**, Calculated interaction energy between a xenon atom and a nanotube as a function of their separation for two different nanotube diameters. **c**, Calculated binding energy as a function of nanotube diameter.

(ref. 19). To understand this difference, we calculated the van der Waals interaction energy between a xenon atom and the different carbon atoms of a nanotube as a function of xenon–nanotube separation (Fig. 4b; Supplementary Section G). The resulting binding energy depends on the nanotube diameter d (Fig. 4c). We obtain $E_b = 133$ meV for $d = 2.2$ nm, in agreement with the measurements. The binding energy is lower than the value reported for graphite, because (i) the nanotube curvature modifies the distance between the xenon atom and the carbon atoms (Fig. 4a, upper inset) and (ii) several graphene layers below the surface of graphite effectively contribute to the long-range van der Waals interaction.

The measurement in Fig. 4a illustrates that adsorption studies[5,6] can be performed on an individual nanotube and with a resolution down to the atomic level (the error bar at low N_{Xe} corresponds to six atoms). Gas adsorption on nanotubes has been the subject of intense research effort because of possible gas storage applications[20–24]. However, previous adsorption measurements were notoriously difficult to interpret, because they were carried out on films of nanotubes, with the atoms being able to diffuse through the film and with the binding energy depending on the different adsorption sites. We avoid these limitations by measuring a single nanotube.

Finally, we discuss the potential applications for nanotube resonators. For surface science research, careful measurements of the noise in the resonance frequency could provide new insights into the diffusion of atoms and molecules along nanotubes[6]. The frequency stability of nanotube resonators might also enable high-sensitivity magnetometry measurements of magnetic nanoscale objects attached to a nanotube[25]. Mass spectrometers based on nanotube resonators might also be able to identify the chemical nature of individual atoms and molecules if single atoms and molecules can be trapped at a specific site on the nanotube (for example, using electrochemistry to create trapping sites by locally modifying the carbon lattice[26]). The shift in the resonance frequency caused by an object landing on a one-dimensional resonator depends on its mass and its position along the resonator, so trapping an object at a known position would allow its mass to be determined directly. Trapping would also reduce fluctuations in the resonance frequency caused by desorption–diffusion.

Methods

Nanotube resonators were fabricated using conventional nanofabrication techniques. Nanotubes were grown by chemical vapour deposition (CVD) on a highly resistive silicon wafer coated with a 1-μm-thick oxide layer. Care was taken to select straight segments of nanotubes by AFM to minimize the slack once the nanotube was suspended[27]. The contact electrodes, and also a side-gate electrode, were patterned using electron-beam lithography and chromium/gold evaporation. The nanotube was suspended over a ~150-nm-wide trench by etching ~50 nm of the oxide with hydrofluoric acid and using a poly(methyl methacrylate) mask. A scanning electron microscopy image of a device at the end of the fabrication process is shown in Fig. 1b.

The device in Fig. 4 was fabricated[15,28] by first patterning the gate electrode in a trench etched in a highly resistive silicon wafer coated with SiO_2 and Si_3N_4. We then fabricated two tungsten/platinum electrodes, separated by the trench. Islands of catalyst particles were deposited on one of the two electrodes, and carbon nanotubes were grown by CVD. Many devices were fabricated on the wafer, and those for which an electrical contact was established between the contact electrodes were chosen for the experiments.

Received 17 January 2012; accepted 29 February 2012; published online 1 April 2012

References

1. Burg, T. P. *et al.* Weighing of biomolecules, single cells and single nanoparticles in fluid. *Nature* **446,** 1066–1069 (2007).
2. Naik, A. K., Hanay, M. S., Hiebert, W. K., Feng, X. L. & Roukes, M. L. Towards single-molecule nanomechanical mass spectrometry. *Nature Nanotech.* **4,** 445–450 (2009).
3. Li, M. *et al.* Nanoelectromechanical resonator arrays for ultrafast, gas-phase chromatographic chemical analysis. *Nano Lett.* **10,** 3899–3903 (2010).
4. Grover, W. H *et al.* Measuring single-cell density. *Proc. Natl Acad. Sci. USA* **108,** 10992–10996 (2011).
5. Wang, Z. *et al.* Phase transitions of adsorbed atoms on the surface of a carbon nanotube. *Science* **327,** 552–555 (2010).
6. Yang, Y. T., Callegari, C., Feng, X. L. & Roukes, M. L. Surface adsorbate fluctuations and noise in nanoelectromechanical systems. *Nano Lett.* **11,** 1753–1759 (2011).
7. Atalaya, J., Isacsson, A. & Dykman, M. I. Diffusion-induced bistability of driven nanomechanical resonators. *Phys. Rev. Lett.* **106,** 227202 (2011).
8. Ekinci, K. L., Yang, Y. T. & Roukes, M. L. Ultimate limits to inertial mass sensing based upon nanoelectromechanical systems. *J. Appl. Phys.* **95,** 2682–2689 (2004).
9. Cleland, A. N. Thermomechanical noise limits on parametric sensing with nanomechanical resonators. *New J. Phys.* **7,** 235 (2005).
10. Yang, Y. T., Callegari, C., Feng, X. L., Ekinci, K. L. & Roukes, M. L. Zeptogram-scale nanomechanical mass sensing. *Nano Lett.* **6,** 583–586 (2006).
11. Lassagne, B., Garcia-Sanchez, D., Aguasca, A. & Bachtold, A. Ultrasensitive mass sensing with a nanotube electromechanical resonator. *Nano Lett.* **8,** 3735–3738 (2008).
12. Chiu, H-Y., Hung, P., Postma, H. W. Ch. & Bockrath, M. Atomic-scale mass sensing using carbon nanotube resonators. *Nano Lett.* **8,** 4342–4346 (2008).
13. Jensen, K., Kim, K. & Zettl, A. An atomic-resolution nanomechanical mass sensor. *Nature Nanotech.* **3,** 533–537 (2008).
14. Gouttenoire, V. *et al.* Digital and FM demodulation of a doubly clamped single-walled carbon-nanotube oscillator: towards a nanotube cell phone. *Small* **6,** 1060–1065 (2010).
15. Eichler, A. *et al.* Nonlinear damping in mechanical resonators made from carbon nanotubes and graphene. *Nature Nanotech.* **6,** 339–342 (2011).
16. Sazonova, V. *et al.* A tunable carbon nanotube electromechanical oscillator. *Nature* **431,** 284–287 (2004).
17. Lassagne, B., Tarakanov, Y., Kinaret, J., Garcia-Sanchez, D. & Bachtold, A. Coupling mechanics to charge transport in carbon nanotube mechanical resonators. *Science* **325,** 1107–1110 (2009).
18. Steele, G. A. *et al.* Strong coupling between single-electron tunneling and nanomechanical motion. *Science* **325,** 1103–1106 (2009).
19. Vidali, G., Ihm, G., Kim, H-Y. & Cole, M. W. Potentials of physical adsorption. *Surf. Sci. Rep.* **12,** 135–181 (1991).
20. Dillon, A. C. *et al.* Storage of hydrogen in single-walled carbon nanotubes. *Nature* **386,** 377–379 (1997).
21. Teizer, W., Hallock, R. B., Dujardin, E. & Ebbesen, T. W. ^{4}He desorption from single wall carbon nanotube bundles: a one-dimensional adsorbate. *Phys. Rev. Lett.* **82,** 5305–5308 (1999).
22. Ulbricht, H., Kriebel, J., Moos, G. & Hertel, T. Desorption kinetics and interaction of Xe with single-wall carbon nanotube bundles. *Chem. Phys. Lett.* **363,** 252–260 (2002).
23. Shi, W. & Johnson, J. K. Gas adsorption on heterogeneous single-walled carbon nanotube bundles. *Phys. Rev. Lett.* **91,** 015504 (2003).
24. Ulbricht, H., Zacharia, R., Cindir, N. & Hertel, T. Thermal desorption of gases and solvents from graphite and carbon nanotube surfaces. *Carbon* **44,** 2931–2942 (2006).
25. Lassagne, B., Ugnati, D. & Respaud, M. Ultrasensitive magnetometers based on carbon-nanotube mechanical resonators. *Phys. Rev. Lett.* **107,** 130801 (2011).
26. Goldsmith, B. R. *et al.* Conductance-controlled point functionalization of single-walled carbon nanotubes. *Science* **315,** 77–81 (2007).
27. Chaste, J., Sledzinska, M., Zdrojek, M., Moser, J. & Bachtold, A. High-frequency nanotube mechanical resonators. *Appl. Phys. Lett.* **99,** 213502 (2011).
28. Hüttel, A. K. *et al.* Carbon nanotubes as ultrahigh quality factor mechanical resonators. *Nano Lett.* **9,** 2547–2552 (2009).
29. Zacharia, R., Ulbricht, H. & Hertel, T. Interlayer cohesive energy of graphite from thermal desorption of polyaromatic hydrocarbons. *Phys. Rev. B* **69,** 155406 (2004).

Acknowledgements

The authors acknowledge support from the European Union through the RODIN-FP7 project, the ERC carbonNEMS project and a Marie Curie grant (no. 271938), the Spanish ministry of science (FIS2009-11284, TEC2009-06986, FIS2009-12721-C04-03, CSD2007-00041) and the Catalan government (AGAUR, SGR). The authors also thank B. Thibeault (UC Santa Barbara) for help with the fabrication.

Author contributions

J.C. fabricated the devices, developed the measurement set-up and performed the measurements. A.E., J.M. and G.C. provided support regarding fabrication, measurement analysis and development of the set-up, respectively. R.R. carried out the calculations of the binding energy. A.B. supervised the work. All authors contributed to discussing the results and writing the manuscript.

Additional information

The authors declare no competing financial interests. Supplementary information accompanies this paper at www.nature.com/naturenanotechnology. Reprints and permission information is available online at http://www.nature.com/reprints. Correspondence and requests for materials should be addressed to A.B.